Development 128, 4217-4227 (2001)
Printed in Great Britain © The Company of Biologists Limited 2001
DEV3512

Abnormal function of astroglia lacking *Abr* and *Bcr* RacGAPs

Vesa Kaartinen[1], Ignacio Gonzalez-Gomez[1], Jan Willem Voncken[1], Leena Haataja[2], Emmanuelle Faure[2], Andre Nagy[1], John Groffen[2,*] and Nora Heisterkamp[2]

[1]Department of Pathology and Laboratory Medicine, Childrens Hospital Los Angeles Research Institute and Keck School of Medicine of the University of Southern California, 4650 Sunset Boulevard, Los Angeles, CA 90027, USA
[2]Division of Hematology and Oncology, Childrens Hospital Los Angeles Research Institute and Keck School of Medicine of the University of Southern California, 4650 Sunset Boulevard, Los Angeles, CA 90027, USA
*Author for correspondence (e-mail: jgroffen@chla.usc.edu)

Accepted 26 July 2001

SUMMARY

Experiments in cultured cells have implicated the molecular switch Rac in a wide variety of cellular functions. Here we demonstrate that the simultaneous disruption of two negative regulators of Rac, *Abr* and *Bcr*, in mice leads to specific abnormalities in postnatal cerebellar development. Mutants exhibit granule cell ectopia concomitant with foliation defects. We provide evidence that this phenotype is causally related to functional and structural abnormalities of glial cells. Bergmann glial processes are abnormal and GFAP-positive astroglia were aberrantly present on the pial surface. Older *Abr;Bcr*-deficient mice show spontaneous mid-brain glial hypertrophy, which can further be markedly enhanced by kainic acid. Double null mutant astroglia are hyper-responsive to stimulation with epidermal growth factor and lipopolysaccharide and exhibit constitutively increased phosphorylation of p38 mitogen-activated protein kinase, which is regulated by Rac. These combined data demonstrate a prominent role for *Abr* and *Bcr* in the regulation of glial cell morphology and reactivity, and consequently in granule cell migration during postnatal cerebellar development in mammals.

Key words: Rac, Bergmann glial cell, External granule cell, Cerebellar development, Null mutant, Mouse

INTRODUCTION

Rac family GTPases act as molecular switches in multiple signaling pathways, including those activated during adhesion and growth factor or cytokine stimulation. Engagement of integrins or stimulation of cells with growth factors leads to increased intracellular levels of RacGTP (del Pozo et al., 2000; Kraynov et al., 2000). The GTP-bound conformation of Rac is its active form, in which it can bind to and further activate downstream effectors (van Aelst and D'Souza-Schorey, 1997; Hall, 1998). Racs cycle between the active GTP-bound state and an inactive GDP-bound state and this is controlled by different classes of modifiers. Guanine nucleotide exchange factors (GEFs) activate Rac, whereas inactivation is promoted by GTPase activating proteins (GAPs). GAPs inactivate Racs by stimulating their intrinsic GTPase activity.

Bcr (breakpoint cluster region) and Abr (active Bcr-related) are two highly related proteins that are expressed at a relatively high level in the central nervous system (CNS) and in hematopoietic tissues (Heisterkamp et al., 1993). Bcr was originally identified because of its involvement in chronic myelogenous leukemia (Groffen and Heisterkamp, 1997). Both proteins contain a domain with homology to that of GAPs for Rac and CDC42. When expressed in vitro, this domain exhibits GAP activity toward Rac and Cdc42 (Heisterkamp et al., 1993; Tan et al., 1993). In addition to the GAP domains, both Abr and Bcr contain GEF (also known as Dbl-homology (DH) domains) and pleckstrin-homology (PH) domains. Although isolated DH-domains of both Bcr and Abr, when bacterially expressed as GST fusion proteins, do display very modest GEF activity toward Rac, Cdc42 and Rho (Chuang et al., 1995), baculovirus-produced full-length proteins, even though they are potent GAPs, do not demonstrate detectable GEF activity toward small GTPases of the Rho subfamily (V. K., N. H. and J. G., unpublished). Moreover, analysis of *Bcr* null mutant hematopoietic cells has confirmed that Bcr functions as a RacGAP in vivo in these cells (Voncken et al., 1995).

Rac family GTPases are also expressed in the CNS, where they have been implicated in the regulation of both neuronal and non-neuronal cell types. In cultured astrocytes, Rac has been shown to be involved in process growth (Kalman et al., 1999). It regulates dendritic and axonal growth, and growth cone function in neuronal cells (Mueller, 1999). Although such studies have provided insight into the possible normal function of Racs in the CNS, they have often relied on the use of exogenously introduced and over-expressed dominant-negative or constitutively active Rac. Such mutated forms of Rac are not present in normal cells, as they are permanently locked in one conformation, whereas naturally occurring Rac cycles between GTP- and a GDP-bound states. In addition, expression levels of endogenous Rac are likely to be carefully regulated, whereas overexpression of mutant Racs is non-physiological and may

interfere with pathways that are not relevant in vivo. This emphasizes the importance of studying the small GTPases and their modifiers, such as GTPase activating proteins, in vivo, i.e. by using gene-targeted animals. That Rac family members and their modifiers are indeed crucial to normal neuronal development and function is further underscored by the recognition that in humans, mutations in oligophrenin (a GAP for Rac, Cdc42 and Rho), Pak3 (an effector of Rac) and ARHGEF6 (an exchange factor for Rac) can lead to non-syndromic X-linked mental retardation (Billuart et al., 1998; Allen et al., 1998; Kutsche et al., 2000).

Despite the prominent expression of *Bcr* in the CNS and in hematopoietic cells, the phenotype of $Bcr^{-/-}$ mice is relatively mild (Voncken et al., 1995). This is not entirely unexpected, because a single highly homologous gene is known, *Abr*, which shows an expression pattern overlapping that of *Bcr*. To elucidate crucial functions of these negative regulators for Rac in vivo, we have therefore generated double null mutant ($Abr^{-/-};Bcr^{-/-}$) mice and have studied the physiological role of Abr and Bcr in the CNS. We find that together, these gene products are essential for the normal functioning of astrocytes, and that their ablation is correlated with concomitant cerebellar developmental defects.

MATERIALS AND METHODS

Generation of *Abr*-deficient mice

The mouse *Abr* locus was cloned from a partial *Mbo*I *B6CBA/F1* genomic library. A targeting vector was constructed by inserting a *PGK-NEO-PA* cassette into an *Nco*I site in *Abr* exon 3, which encodes an N-terminal fragment of the DH domain (residues 70-131, Heisterkamp et al., 1993). An *HSV-TK* cassette was introduced into the non-homologous region of the construct. The structure of the targeting vector is shown in Fig. 1A. Insertion of a *PGK-NEO-PA* cassette introduces several STOP-codons in all three reading frames and results in the putative generation of a truncated protein product consisting of the 80 amino acids encoded by the first two exons and by a part of exon 3. The targeting vector (30 μg) was linearized with *Xho*I and introduced into R1 embryonic stem cells (1×10^7 cells) by electroporation (230V/580 mF). Transfected cells were seeded onto neo^r STO feeder cells, and double selection (200 μg/ml $G418^R$; 2 μM ganciclovir) was started 24 hours after electroporation (Kaartinen et al., 1995; Voncken et al., 1995). Double-drug-resistant colonies were picked 8-11 days after electroporation and expanded as described (Wurst and Joyner, 1993). Cell lines and tail DNAs were screened for the presence of a disrupted *Abr* allele by Southern blot analysis using *Hin*dIII digestion and hybridization with an external probe. The frequency of correct targeting at the *Abr* locus was 1 in 96 double-resistant clones. Clone 52.1, which contained the correct recombination in the *Abr* gene, was used to obtain chimeric males. These were bred with Black Swiss female mice and heterozygous offspring were interbred to generate homozygous offspring.

Generation of *Abr;Bcr* double mutant mice

Double knockout ($Abr^{-/-};Bcr^{-/-}$) mice were generated by crossing *Abr* homozygotes (50% 129Sv and 50% Black Swiss) with *Bcr* homozygotes (50% 129Sv and 50% C57BL/6; Voncken et al., 1995). Double heterozygotes were subsequently interbred to obtain double homozygotes. In all experiments, littermates were used as controls for $Abr^{-/-};Bcr^{-/-}$ double null mutants.

Generation of Bcr-DH-PH transgenic mice

The transgenic construct was generated from a human genomic DNA fragment encompassing the entire *BCR* promoter, exon 1 encoding the Serine/Threonine kinase domain plus pieces of flanking introns, as well as the exons encoding the DH and PH domains. The GAP domain in Bcr is from amino acid residues 1074 to1216. To generate the C-terminal end, we filled in a *Pst*I site around amino acid residue 1250 and ligated it to a *Pvu*II site at around amino acid residue 953. The generated construct encodes a protein that misses amino acid residues 953-1250, but contains residues 1251-1271, and the natural stop codon and 3′ untranslated sequences. Mice transgenic for the *BCR-DH-PH* construct were generated at the NICHD transgenic mouse development facility at the University of Alabama at Birmingham. Transgenic double null mutants were generated by breeding transgenic mice to the double null mutant background until desired genotypes were obtained.

Histological studies

Tissues were fixed by intracardiac perfusion with 4% paraformaldehyde, processed and embedded in paraffin. For standard histology, sections were cut at 5 μm and stained with Hematoxylin and Eosin. Paraformaldehyde fixed sections were stained with primary antibodies to calbindin (Sigma), GFAP (Zymed) and synaptophysin (Sigma) using a Histomouse kit according to the manufacturer's instructions (Zymed). Golgi staining was carried out as described previously (Angulo et al., 1996). For in situ hybridization analysis, 10 μm sections were prepared and processed following the manufacturer's protocol for digoxigenin-labeled oligonucleotide probes (Boehringer Mannheim). Fragments of murine *Abr*, including exons 2-4 and of murine *Bcr* (Fioretos et al., 1995) encompassing a similar region, were used as probes. For some immunohistochemical staining, tissues were sectioned using a vibratome and immunostained for GFAP (DAKO) and S100 (DAKO) according to standard procedures. For nestin and RC2 staining, newborn brains were frozen in isopentane and frozen tissues were sectioned to a thickness of 15 μm. The nestin (rat-401) antibodies developed by S. Hockfield and RC2 antibodies developed by M. Yamamoto were obtained from the Developmental Studies Hybridoma Bank developed under the auspices of the NICHD and maintained by the University of Iowa, Department of Biological Sciences, Iowa City, IA. The area encompassing the internal granule cell layer (IGL) layers in folia III-V was analyzed using MetaMorph^R software (Universal Imaging Corporation™).

Granule cell cultures

Cerebellar granule neurons and astroglia were isolated as described (Hatten, 1985). To study granule cell-astroglial interactions, GFAP-positive astroglial cells were plated onto poly-L-lysine coated chamber slides (50,000 per 2 cm^2). A fivefold excess of granule cells was added, and the cells were incubated for 4 days at 35.5°C with 100% humidity in 5% CO_2. The number of astroglial processes and their length was scored under a phase-contrast microscope. Granule cell apoptosis was assayed as described previously (Spector et al., 1997).

Electron microscopy

Tissues were fixed by intracardiac perfusion with 2.5% glutaraldehyde and 0.1 M potassium phosphate, pH 7.4, postfixed with 1% osmium tetroxide and embedded in epoxy resin. Specimens were stained with uranylacetate and lead citrate and examined with a Philips CM-12 transmission electron microscope.

Astroglial cultures

Cerebellar astroglia were isolated from newborn mice as described (Hatten, 1985). GFAP-positive astroglial cells were plated onto poly-L-lysine and fibronectin coated chamber slides (50,000 per 2 cm^2). For epidermal growth factor (EGF)-mediated stimulation and immunofluorescence, cell were serum-starved and treated with 25 ng/ml of EGF for 24 hours. Cells were subsequently fixed with 2%

paraformaldehyde and stained for GFAP (DAKO) and actin (FITC-labeled phalloidin from Sigma). Rabbit polyclonal anti-GFAP antibodies were detected using Cy3-labelled goat anti-rabbit antibodies (Jackson Immuno Research). Slides were analyzed using a Leica TCS SP laser scanning microscope. Cell spreading was analyzed using MetaMorph^{R} software (Universal Imaging Corporation™).

Cerebellar slice cultures and BrdU labeling

Cerebella from P5 mice were removed, embedded in 2% agarose, cut into 300 mm thick sagittal sections and cultured and analyzed for BrdU incorporation as described (Wechsler-Reya and Scott, 1999).

Activation of MAPK pathways

Astroglial cultures were established as described above and expanded in basal medium Eagle containing 10% fetal calf serum and 5% horse serum. Stimulation with lipopolysaccharide (LPS) took place at a concentration of 1 μg/ml. For EGF stimulation, cells were first serum starved for 20 hours and subsequently stimulated with 25 ng/ml of EGF. Cells were harvested in 2× Laemmli sample buffer and analyzed for p38 mitogen-activated protein kinase (MAPK) phosphorylation using standard western blot analysis. Phospho-specific p38MAPK, pJNK and pERK antibodies were from Cell Signaling Technology. Antibodies for p38 MAPK, JNK and ERK were from Santa Cruz Biotechnology. The results were analyzed using the Un-Scan-It program (Silk Scientific).

Rac activation assay

Thioglycollate elicited peritoneal monocytes were lysed as described (Benard et al., 1999). Lysates were incubated with GST-PAK (PAK CRIB-domain) and affinity-precipitated proteins were separated by SDS-polyacrylamide gel electrophoresis, followed by immunoblotting with anti-Rac antibodies (Transduction Laboratories). Filters were stripped and re-incubated with anti-CDC42 antibodies (Santa Cruz Biotechnology). The results were analyzed using Un-Scan-It software (Silk Scientific).

RESULTS

Generation of *Abr;Bcr* double null mutants

Homologous recombination in embryonic stem cells was used to create a mouse strain, in which the *Abr* gene was disrupted in exon 3 (Fig. 1A). Immunoblotting confirmed the absence of an *Abr* gene product in *Abr*$^{-/-}$ mice (Fig. 2A and results not shown; the faint bands in knockout samples are proteins that react non-specifically with the polyclonal antiserum and were not seen with antibodies that recognize only the 96 kDa form). These phenotypically normal animals were crossed with *Bcr*$^{-/-}$ mice (Voncken et al., 1995). Breeding of double heterozygotes (*Abr*$^{+/-}$;*Bcr*$^{+/-}$) yielded viable double null mutants, albeit at reduced frequency. This was due to perinatal lethality, because if genotyping was done immediately after birth, the expected number of double knockouts was obtained. Already prior to postnatal day 10, double homozygotes could be easily distinguished from their littermates because of clumsy movements. Adults also often stumbled and showed additional abnormal behavior, consisting of hyperactivity and persistent

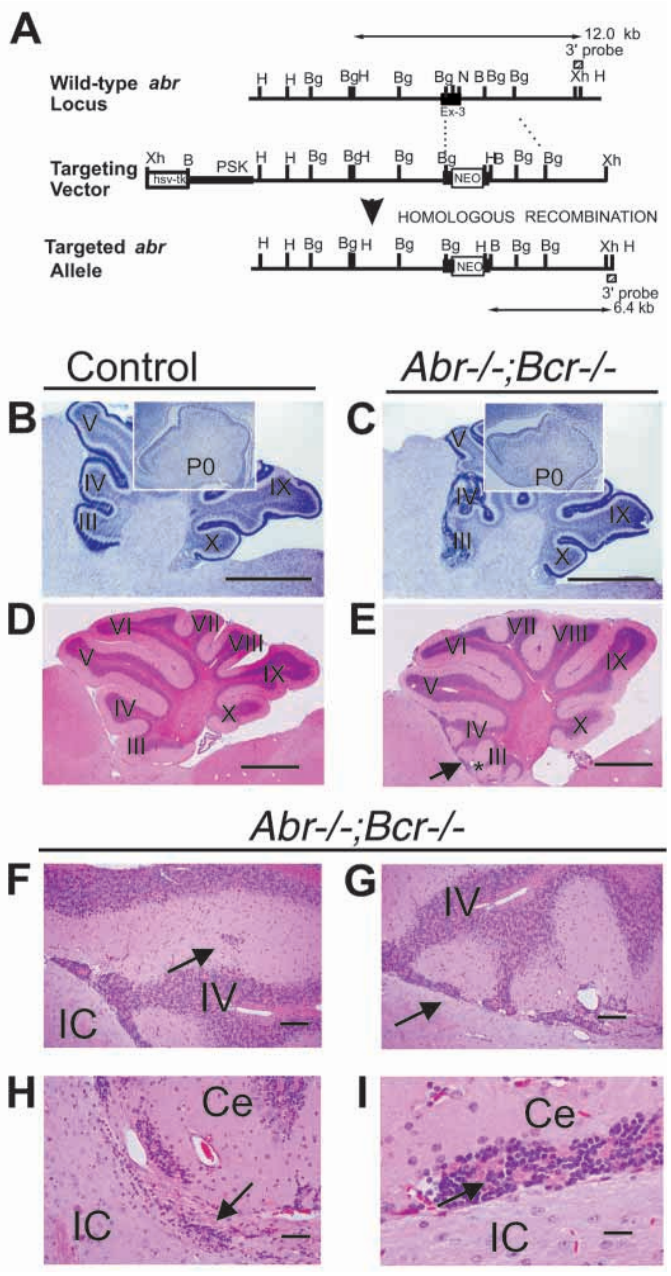

Fig. 1. Double knockout (*Abr*$^{-/-}$;*Bcr*$^{-/-}$) mice display abnormal cerebellar development. (A) Schematic drawing of the wild-type *Abr* locus, the targeting vector and the mutant allele. The targeting vector was constructed by inserting a PGK-neo-pA cassette into the *Nco*I site of exon 3. The hatched box represents the *Xho*I-*Hin*dIII fragment which was used as an external 3′ probe. The predicted sizes of *Hin*dIII fragments hybridizing to this probe are shown above the wild-type locus and below the targeted locus. Restriction enzymes: H, *Hin*dIII; Bg, *Bgl*II; N, *Nco*I; B, *Bam*HI; Xh, *Xho*I. (B-E) Hematoxylin and Eosin stained midsagittal sections through wild-type (B,D) and double null mutant cerebellum (C,E). Samples were taken at 11 days (B,C; insets at postnatal day 0) and 3 months (D-I) of age. Note abnormal foliation (E, asterisk) and the presence of persistent granule cells on the surface of the molecular layer (E, arrow). (F-I) The double knockout specimens display fusion of folia (F, arrow), abnormal foliation (G) in the anterior folia (III and IV) of the cerebellum, and presence of abnormal ectopic granule cells (G-H, arrows) when compared with age-matched wild-type controls. There was a rosette-like arrangement of the ectopic granule cells around an eosinophilic fibrillary core (I, arrow). Vermal folia are indicated with roman numerals, III-X. Anterior is towards the left of each photograph. Ce, cerebellum; IC, inferior colliculus. Scale bars: 1 mm in B-E; 300 μm in insets of B,C; 100 μm in D-H; 50 μm in I.

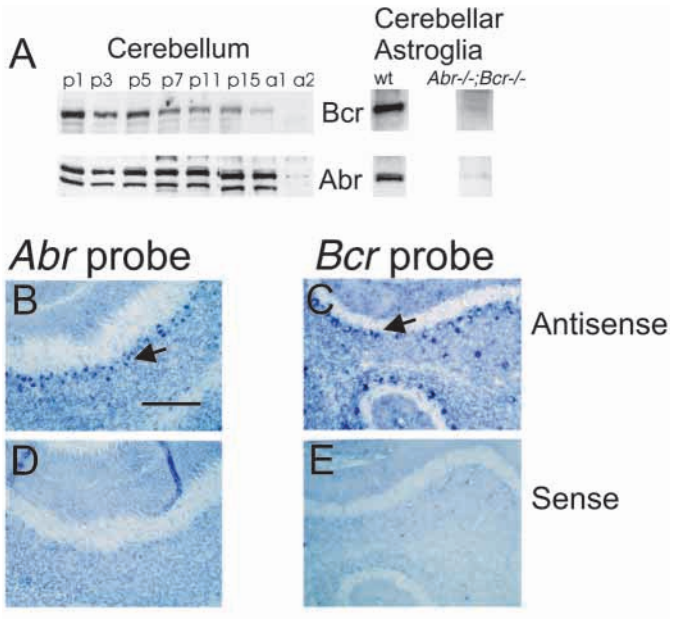

Fig. 2. *Abr* and *Bcr* are expressed in the postnatal cerebellum. (A) Bcr and Abr protein levels were examined in the cerebellum at P1-15, in adult wild-type cerebellum (a1), in adult $Abr^{-/-};Bcr^{-/-}$ cerebellum (a2) and in primary cerebellar astrocytes isolated at P0. In total cerebellar extracts, two forms (96 kDa and 91 kDa) of Abr are present, whereas cultured astrocytes express only the smaller 91 kDa form. Null mutants lacked both 96 and 91 kDa forms but the antiserum used aspecifically reacts with proteins in that size range. (B-E) In situ hybridization of wild-type midsagittal sections of the cerebellum at the age of 8 days using *Abr* (B,D;, left panel) and *Bcr* (C,E, right panel) probes. (B,C) Anti-sense probes. (D,E) Sense probes used as a negative control. Arrows in B,C point to intensely stained Purkinje cells. Scale bars: 150 μm.

circling. Some of these phenotypic features, which are associated with vestibular dysfunction of the inner ear, could be attributed to the absence of vestibular octoconia in these animals (currently under investigation). However, the early postnatal motoric impairment also inspired us to study the central nervous system and particularly the cerebellum, which is involved in motor control, in more detail.

Granule cell ectopia in *Abr;Bcr* double null mutants

When the cerebella of adult double null mutants were compared with those of control littermates, large numbers of granule neurons were found in an abnormal location on the surface of the molecular layer of the cerebellum, both in the vermis as well as in both hemispheres of all double null mutants (Fig. 1E). In adult controls, such granule neurons are located exclusively in the internal granule cell layer (IGL) of the cerebellum (see Fig. 1D). In double null mutants, the ectopic cells could be found in all folia, but their number was strikingly high in the anterior folia of the cerebellar vermis and anterior medullary velum (Fig. 1E-H and data not shown). This phenotype was associated with an abnormal anterior foliation pattern including partial fusion (Fig. 1F) and was 100% penetrant in double knockouts, but was never found in wild type or single knockouts (either $Abr^{-/-}$ or $Bcr^{-/-}$).

Cerebellar development mainly occurs within the first three postnatal weeks, and is characterized by extensive neuronal outgrowth and migration. During this period, granule cells located on the surface of the cerebellum (see Fig. 1B,C) in the so-called external granule layer (EGL) migrate inward toward their final destination in the IGL underneath the Purkinje cell layer (see Fig. 1D,E).

We therefore analyzed young animals. The defective foliation was distinctly detectable as early as p11 (Fig. 1C), when the migration of cerebellar granule neurons is actively ongoing, whereas newborn double null mutants did not display detectable differences in their cerebellum when compared with control littermates (Fig. 1B,C, insets). Tension generated along granule cell axons, the parallel fibers, has been suggested as an explanation for why the cerebellar cortex folds in a characteristic species-specific pattern (van Essen, 1997). Indeed, in the double null mice, defective foliation was obvious in locations where the most prominent amounts of ectopic granule cells could be found, suggesting that the defect in foliation is secondary to the presence of ectopic granule cells in the molecular layer.

Abr and Bcr are expressed in major cell types in the cerebellum

To correlate the observed abnormal cerebellar development with lack of *Abr* and *Bcr*, we studied their expression in the cerebellum during the crucial time span of p1-p15. This analysis showed that both are expressed during this entire period (Fig. 2A). Two major cerebellar neuronal types are Purkinje and granule cells. Both *Abr* and *Bcr* were found to be strongly expressed in Purkinje cells in pups at p8 (Fig. 2B-E) and in adults (data not shown). Bcr and Abr were also present in granule cells (not shown). Astroglial primary cultures established at p0 additionally showed consistent expression of both proteins (Fig. 2A). These results indicate that the primary cause of the defects observed in the double null mutant cerebellum coincides with lack of *Abr* and *Bcr* in several distinct cerebellar cell types.

Purkinje and granule cells of *Abr;Bcr* double null mutants are phenotypically normal

Several possible explanations were considered to account for the presence of the ectopic granule cells. Studies with numerous mouse mutants have shown that granule cell number and migration is correlated with the organization and number of the underlying Purkinje cells, on which the granule cells synapse. It has also been shown that loss of Purkinje cells results in a concomitant reduction in the size of the granule cell population and defects both in lamination and foliation (Goldowitz and Hamre, 1998). In addition, expression of constitutively active Rac1 in Purkinje cells of transgenic mice leads to a significant reduction in the number of Purkinje cell axon terminals in the deep cerebellar nuclei, and a reduction in size but an increase in number of Purkinje cell dendritic spines (Luo et al., 1996).

However, in the *Abr;Bcr* double null mutants, we found that the dendritic trees of Purkinje cells also showed a high degree of complexity in the anterior folia and contained clearly detectable spines, similar to controls (Fig. 3A-D). Moreover, the Purkinje cell axon terminals of double knockout mice were indistinguishable from those of controls (data not shown). The affected anterior folia of most double mutants contained Purkinje cells which were morphologically and numerically indistinguishable from controls (Fig. 3E,F).

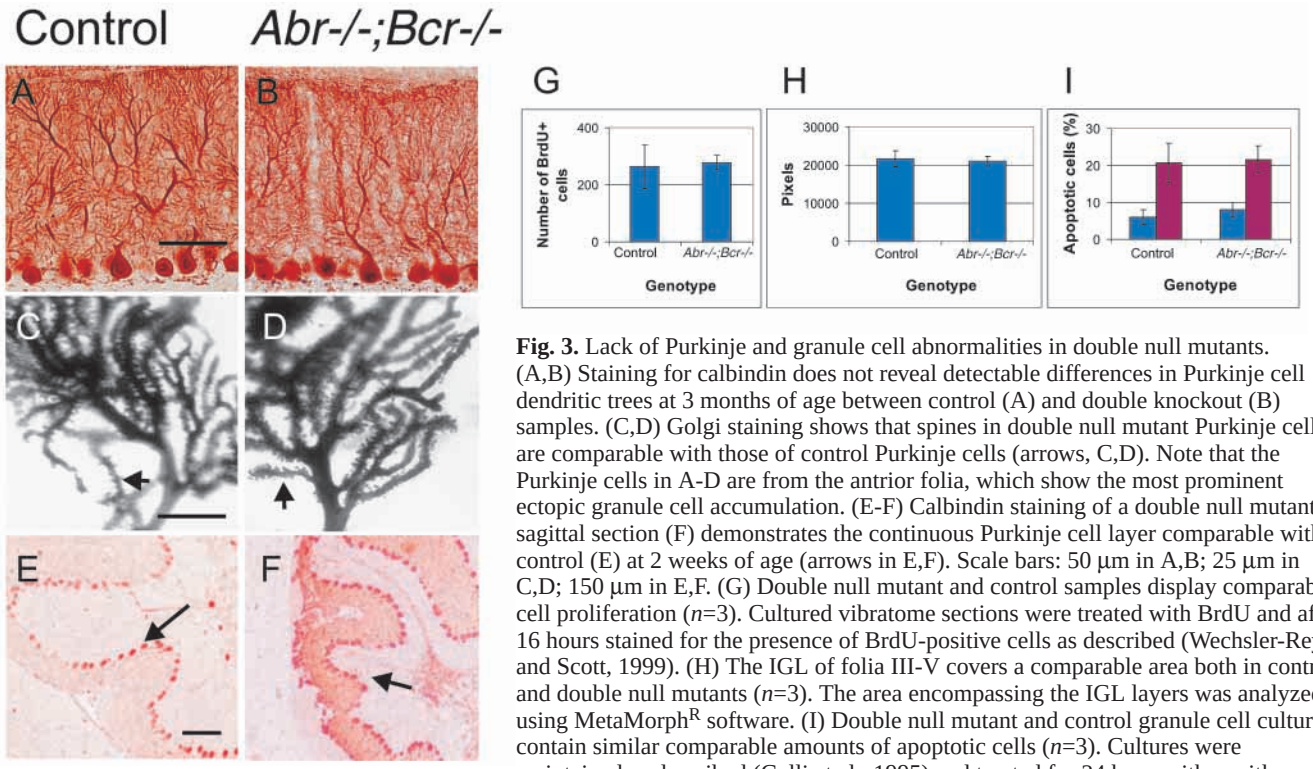

Fig. 3. Lack of Purkinje and granule cell abnormalities in double null mutants. (A,B) Staining for calbindin does not reveal detectable differences in Purkinje cell dendritic trees at 3 months of age between control (A) and double knockout (B) samples. (C,D) Golgi staining shows that spines in double null mutant Purkinje cells are comparable with those of control Purkinje cells (arrows, C,D). Note that the Purkinje cells in A-D are from the antrior folia, which show the most prominent ectopic granule cell accumulation. (E-F) Calbindin staining of a double null mutant sagittal section (F) demonstrates the continuous Purkinje cell layer comparable with a control (E) at 2 weeks of age (arrows in E,F). Scale bars: 50 μm in A,B; 25 μm in C,D; 150 μm in E,F. (G) Double null mutant and control samples display comparable cell proliferation (n=3). Cultured vibratome sections were treated with BrdU and after 16 hours stained for the presence of BrdU-positive cells as described (Wechsler-Reya and Scott, 1999). (H) The IGL of folia III-V covers a comparable area both in controls and double null mutants (n=3). The area encompassing the IGL layers was analyzed using MetaMorph^R software. (I) Double null mutant and control granule cell cultures contain similar comparable amounts of apoptotic cells (n=3). Cultures were maintained as described (Galli et al., 1995) and treated for 24 hours either with 25 mM KCl in the presence of serum (protected against apoptosis, blue columns) or with 5 mM KCl in the absence of serum (apoptosis induced, red columns). The number of apoptotic cells was analyzed using FACS as described (Spector et al., 1997).

It has recently been shown that granule cell proliferation and differentiation are tightly regulated by Purkinje cell-derived Sonic hedgehog (Shh), and that inhibition of Shh signaling leads to an abnormal development of Purkinje and granule cells (Wechsler-Reya and Scott, 1999; Dahmane and Ruiz-i-Altabe, 1999). However, we did not detect clear differences in Shh levels between double null mutants and controls at 5 and 10 days of age (data not shown). Moreover, BrdU staining on slice cultures did not demonstrate detectable differences in granule cell proliferation (Fig. 3G) and the number of internal granule cells appeared grossly comparable between double knockouts and wild-type controls. In wild-type controls, the IGL of folia III-V covered a relative area comparable to that of double null mutants (Fig. 3H). Moreover, in double null mutants the number of apoptotic granule cells both in the presence (blue columns, Fig. 3I) and absence (red columns, Fig. 3I) of depolarizing potassium concentrations was comparable with that of controls, and in double null mutants, granule cells formed normal synapses with mossy fibers (data not shown). Together these results show that the presence of the ectopic granule cells could not easily be explained by either Purkinje cell or granule cell abnormalities.

Abr;Bcr double null mutants display aberrant GFAP-positive astroglia on the surface of the EGL layer at p5

The directed migration of the granule cells from the surface of the molecular layer to their final destination just underneath the Purkinje cell layer is guided by and is dependent upon glial processes of the Bergmann glial cells (Golgi cells; Hatten, 1990). For example, loss of meningeal cells of the cerebellum by treatment of newborn rats with 6-OHDA results in disruption of the glial scaffold and in abrogation of granule cell migration (von Knebel Doeberitz et al., 1986). Therefore, we considered possible abnormalities of these glial cells as an alternative explanation for the presence of the ectopic granule cells.

During the first two postnatal weeks, Bergmann glia undergo progressive maturation, which is accompanied by changes in intermediate filament (IF) protein expression (Yuasa, 1996). To characterize double null mutant Bergmann glia, we first stained mutant and control specimen at postnatal day 1 using anti-nestin and RC2 antibodies, which detect the IF protein nestin and an IF-associated protein, respectively, in immature fibers but not in mature Bergmann glia (Mission et al., 1988; Dahlstrand et al., 1995). However, we could not see detectable differences in positively staining fibers on the cerebellar cortex between controls and double null mutants at postnatal day 1 (Fig. 4), suggesting that early development of *Abr*$^{-/-}$*;Bcr*$^{-/-}$ Bergmann glia does not significantly deviate from that of controls.

After postnatal day 4, maturing Bergmann processes stain positive for glial fibrillary acidic protein (GFAP). Immunostaining for GFAP at p5 demonstrated the presence of radial Bergmann processes both in controls and in double null mutants (Fig. 5). In controls, the glial processes extended from the Purkinje cell layer to the pial surface, where their end-feet formed a continuous glial boundary (Fig. 5A,D). In double null mutants however, the glial processes often lost their radial orientation when they approached the pial surface and displayed abnormal end-feet, that failed to form a well-defined glial boundary (Fig. 5E, arrows and inset). Other glial processes abnormally penetrated the intrafissural space (Fig. 5B,C, arrows).

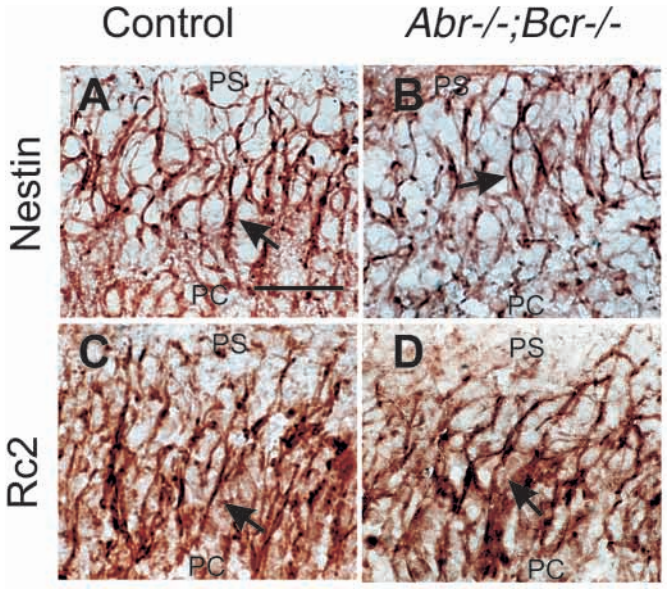

Fig. 4. Immature Bergmann glia are indistinguishable between double null mutants and controls at p1. Immunostaining using nestin (A,B) and RC2 (C,D) antibodies shows that immature double null mutant Bergmann protrusions (B,D) do not differ from immature control protrusions (A,C) at P1. Arrows point to positively staining protrusions. PS, pial surface; PC, Purkinje cell layer. Scale bars: 20 μm.

The normal somata of Bergmann glial cells as well as their processes can be visualized by staining for the S100 marker. Immunostaining for S100 confirmed the presence of positively staining Bergmann processes, as well as their somata, underneath the Purkinje cell layer, both in controls and in double null mutants (Fig. 5F-I). However, in the double null mutants, S100-positive staining was also observed in an abnormal location, underneath the pial surface (arrows Fig. 5G,I).

To confirm and extend these observations, we performed confocal microscopy on wild-type and double null mutant samples stained for GFAP and calbindin. Whereas the wild-type cerebellum at P5 and P8 showed well-organized and radially oriented Bergmann processes that terminated in a well-defined layer at the pial surface (Fig. 6A,C), the *Abr;Bcr* double mutant samples looked strikingly different. This analysis confirmed the premature termination and disorganization of the end-feet of the Bergmann fibers in these samples (Fig. 6B,D). As shown in Fig. 6B,D, the pial surface also contained aberrant GFAP-positive astrocytes. These possessed long Bergmann-like processes that extended towards the Purkinje cell layer, indicating that they were not typical stellate astrocytes (Fig. 6D inset, arrowhead).

This analysis shows that at P5, the double null mutants already displayed abnormal Bergmann processes in addition to aberrant Bergmann glial-like cells in those locations, in which granule cell ectopia is present after granule cell migration. The Bergmann-like cells have long protrusions that, together with the abnormal Bergmann processes themselves, are likely to

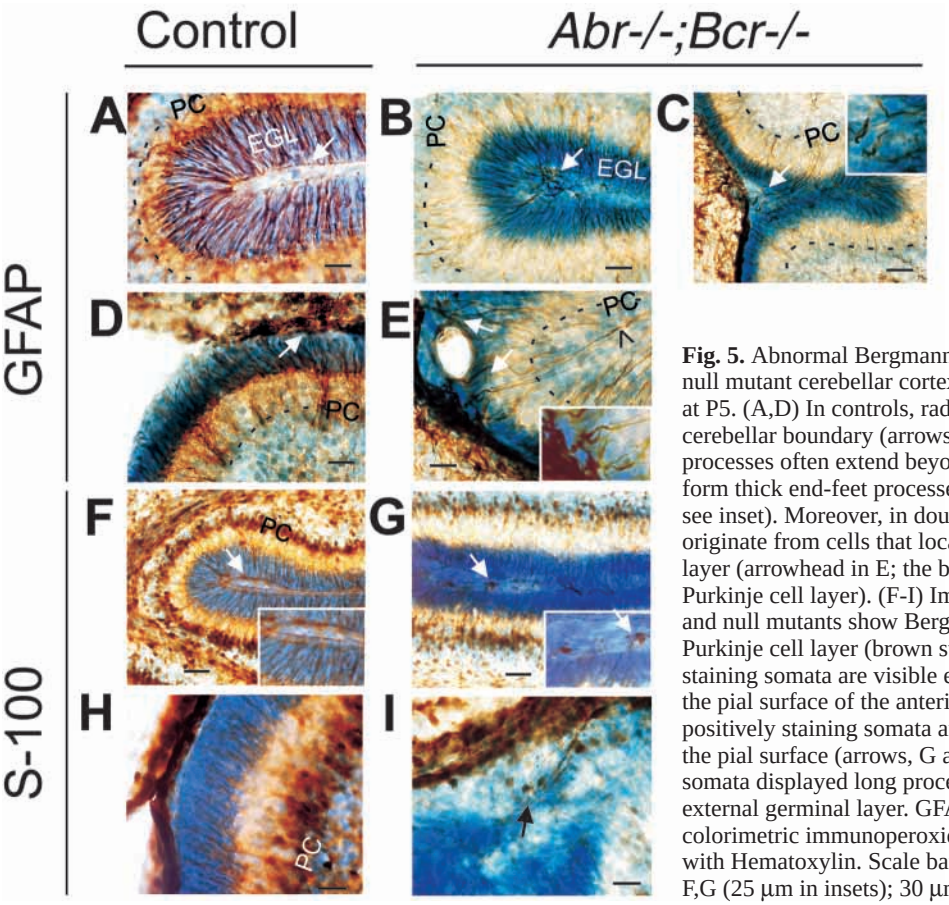

Fig. 5. Abnormal Bergmann processes and aberrant astroglia in double null mutant cerebellar cortex after P5. **(**A-E) Immunostaining for GFAP at P5. (A,D) In controls, radial Bergmann processes form a well-defined cerebellar boundary (arrows). (B,C,E) In double mutants, Bergmann processes often extend beyond the pial surface (arrows in B,C), or they form thick end-feet processes without reaching the pial surface (E, also see inset). Moreover, in double null mutants, Bergmann processes often originate from cells that locate underneath the Golgi-cell/Purkinje-cell layer (arrowhead in E; the broken line indicates the position of the Purkinje cell layer). (F-I) Immunostaining for S100 at p5. Both control and null mutants show Bergmann processes and somata underneath the Purkinje cell layer (brown staining). (F,H) In controls, no positively staining somata are visible either in the intrafissural space (F, inset) or on the pial surface of the anterior lobes (H). (G,I) In double null mutants, positively staining somata are present in the intrafissural space and on the pial surface (arrows, G and inset). Occasionally, these S100-positive somata displayed long processes (arrow, I). PC, Purkinje cell layer; EGL, external germinal layer. GFAP and S100 were detected using a colorimetric immunoperoxidase reaction. Cells were counter-stained with Hematoxylin. Scale bars: 30 μm in A-E (15 μm in insets); 50 μm in F,G (25 μm in insets); 30 μm in H,I.

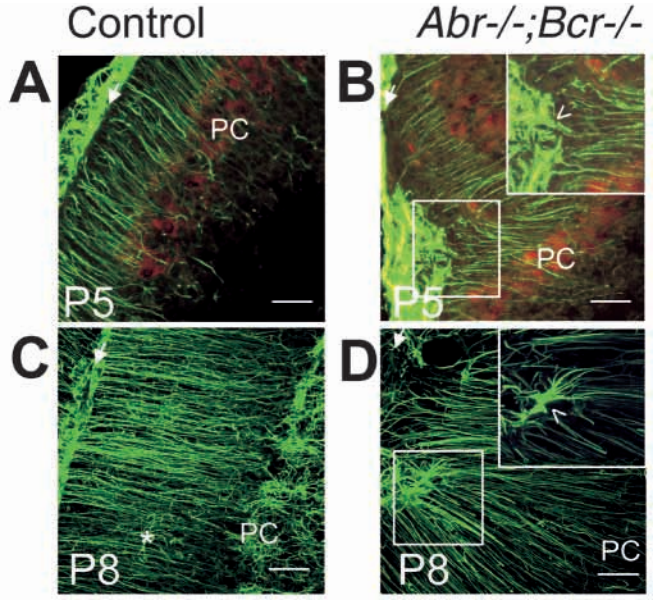

Fig. 6. Confocal microscopy analysis shows disorganization of Bergmann fibers and long processes of abnormal GFAP-positive astroglia in double null mutants. **(**A,C) Wild types at P5 (A) and p8 (C) display well-organized Bergmann processes with an exclusively radial orientation and well-defined end-feet (arrows). (B,D) By contrast, *Abr;Bcr* double null mutant Bergmann processes show disorganization close to the pial surface both at P5 (B) and P8 (D). In addition, double null mutants show the presence of aberrant glial cells on the pial surface (arrowheads in insets) which display long thin processes similar to Bergmann processes (inset D, arrowhead). Arrows point to the pial surface. Immunostaining for GFAP and detection of FITC immunofluorescence (green) was performed using confocal microscopy. Purkinje cells were stained with calbindin and detected by TRITC immunofluorescence (red) in the images on the left. Scale bar: 30 μm A,C (15 μm inset); 50 μm B,D (25 μm inset).

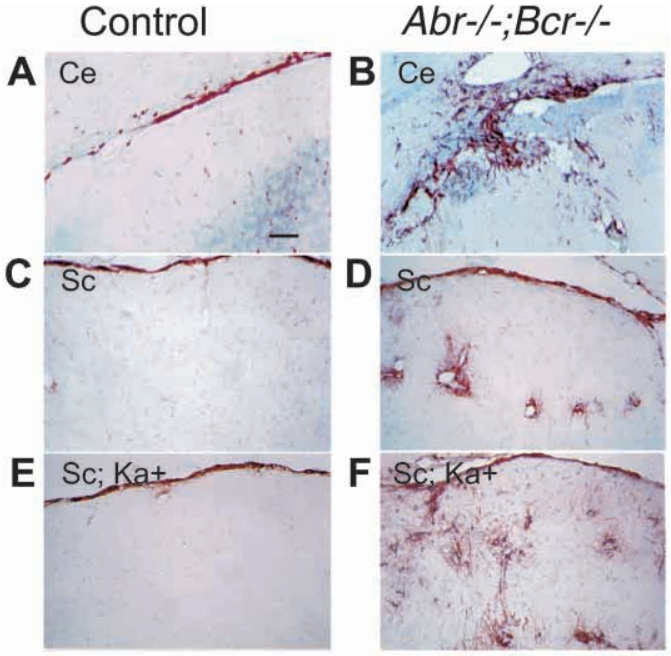

Fig. 7. Glial hypertrophy in the anterior cerebellum and midbrain of adult *Abr;Bcr* double null mutants. (A,B) In the anterior cerebellum of double null mutants, the ectopic granule cells are surrounded by numerous GFAP-positive glial cells (B), whereas in controls, a similar staining is absent (A). (C,D) Glial hypertrophy is also present in the midbrain of adult *Abr;Bcr* mutants (D) but not in controls (C). (E) Control midbrains show no detectable glial hypertrophy upon exposure to kainic acid. (F) Treatment of double null mutants with kainic acid results in massive gliosis in the midbrain. Ce, cerebellum; Sc, superior colliculus; KA, kainic acid. Scale bars: 100 μm in A,B; 50 μm in C-F.

interfere with normal granule cell migration and thus cause the observed granule cell ectopia.

Reactive gliosis in double null mutant midbrain

As the cerebella of young double null mutants contained abnormal, GFAP-positive astroglia, we also analyzed adult mutants for GFAP expression. As shown in Fig. 7B, adult double null mutants displayed a large number of GFAP-positive astroglia adjacent to the ectopic granule cells in the cerebellum. The glial hypertrophy was not associated with neuronal cell death (data not shown). In addition, intense GFAP immunostaining was detected in the superior colliculus of *Abr;Bcr* double null mutants but not in those of controls at the age of 3 months (compare Fig. 7C with 7D).

Whereas the astroglia in the midbrain of control mice did not significantly respond to exposure to the excitotoxic glutamate receptor agonist kainic acid (Fig. 7E), in the double null mutants, a robust increase in the level of GFAP staining was apparent (Fig. 7F). Unlike the hippocampus, in which kainic acid is known to induce rapid neuronal cell death, the midbrain did not show neuronal loss either in the controls or in the double mutants. Thus, in the double knockouts, excessive neuronal damage was not correlated with and did not appear causative for the spontaneous hypertrophy of glial cells in the cerebellum of older animals and the kainic acid-induced gliosis in the midbrain.

Abr;Bcr-deficient astrocytes from mid and hind brain show increased spreading and p38 MAPK phosphorylation in vitro

We have previously shown that Bcr acts as an important negative regulator of Rac in phagocytic cells in vivo (Voncken et al., 1995). In such cells, it downregulates production of reactive oxygen species (ROS) by the NADPH oxidase complex though Rac. Neutrophils of *Bcr*-deficient mice demonstrate a pronounced increase in ROS production and exposure of $Bcr^{-/-}$ mice to Gram-negative endotoxin leads to severe, neutrophil-meditated septic shock and tissue injury (Voncken et al., 1995). Recent evidence indicates that, in addition to phagocytic cells, reactive oxygen intermediates produced by the NADPH-oxidase also play an important role in non-phagocytic cells, including astroglia, in which they act as second messengers (Robinson et al., 1999).

Thus, we considered the possibility that the activation of astroglia in *Abr;Bcr* double null mutants results from increased ROS production in these cells. However, in primary astrocyte cultures, baseline as well as PMA-induced ROS production was at a comparable level in both control and mutant cells (data not shown).

Apart from ROS production, Rac proteins are also involved in regulation of other signals downstream of cytokine and growth factor receptors. It is well established that Racs regulate the kinase cascades that result in phosphorylation and

activation of Jun N-terminal kinase (JNK) and the related p38 MAPK. Upon activation, these kinases translocate to the nucleus, where they phosphorylate transcription factors, such as Jun, ATF2, ELK and Max (van Aelst and D'Souza-Schorey, 1997). In other experiments, we found that double null mutant monocytes had significantly higher levels of phopho-p38 MAPK than did wild type. We therefore compared the phosphorylation status of JNK and p38 MAPK in control and *Abr;Bcr*-deficient astrocytes. Interestingly, in the presence of 10% fetal calf serum and 5% horse serum, double null mutant astrocytes showed a baseline level of p38 phosphorylation that was approx. threefold higher than that of wild-type controls (Fig. 8A, lower panel, 0 time points), whereas no differences could be detected in JNK and in extracellular-regulated kinase (ERK) phosphorylation between the two genotypes (data not shown). In the absence of serum, the double mutants displayed a lower baseline level of p38 MAPK phosphorylation than controls (Fig. 8A, upper panel, 0 time points). This result indicates that the double null astrocytes are hyper-responsive to serum.

Recently, it has been shown that EGF receptor-deficient mice display abnormal CNS development, with a delay in the formation or in the migration of GFAP-positive astrocytes (Kornblum et al., 1998). Moreover, it has been shown that basic fibroblast growth factor (FGF) and EGF induce processes in hippocampal CA1/CA3 astrocytes (Kalman et al., 1999). Therefore, we compared the effect of stimulation with EGF on JNK and p38 MAPK phosphorylation and on possible morphological changes in double null mutant and control astrocytes. Serum-starved, double null mutant primary astrocytes responded to EGF stimulation with a significant and progressive phosphorylation of p38 MAPK, whereas controls showed barely detectable responses (Fig. 8A, top panels). We could not detect significant differences in JNK phosphorylation between double null mutants and controls. We also analyzed the morphology of these cells without and upon stimulation with EGF for 24 hours. During this period, EGF stimulation of the astrocytes did not lead to a significant increase in cell numbers when compared with the non-treated cultures. Serum starved, unstimulated double null mutant cells were ~20% more spread than control cells treated in the same manner (Fig. 8B,C and data not shown). In addition, upon EGF stimulation, some $Abr^{-/-};Bcr^{-/-}$ cells projected distinct GFAP-positive protrusions that were not seen in EGF-stimulated control astrocytes (compare Fig. 8B,C, right panels).

It has recently been described, that although astrocytes lack CD14 LPS receptors, they still respond to LPS stimulation by p38 MAPK phosphorylation (Schumann et al., 1998). This was explained by the fact that p38 activation takes place only in the presence of serum, which provides a soluble form of CD14. CD14, when complexed with LPS, has been shown to activate a cell surface receptor, TLR4 (Toll-like receptor 4), and subsequently a set of complex signaling cascades, in which Racs have also been shown to play an important role (Aderem and Ulevitch, 2000; O'Neill, 2000). Therefore, we compared the responses of control and *Abr;Bcr* null mutant astrocytes with LPS stimulation. As shown in Fig. 8A (bottom panels) double null

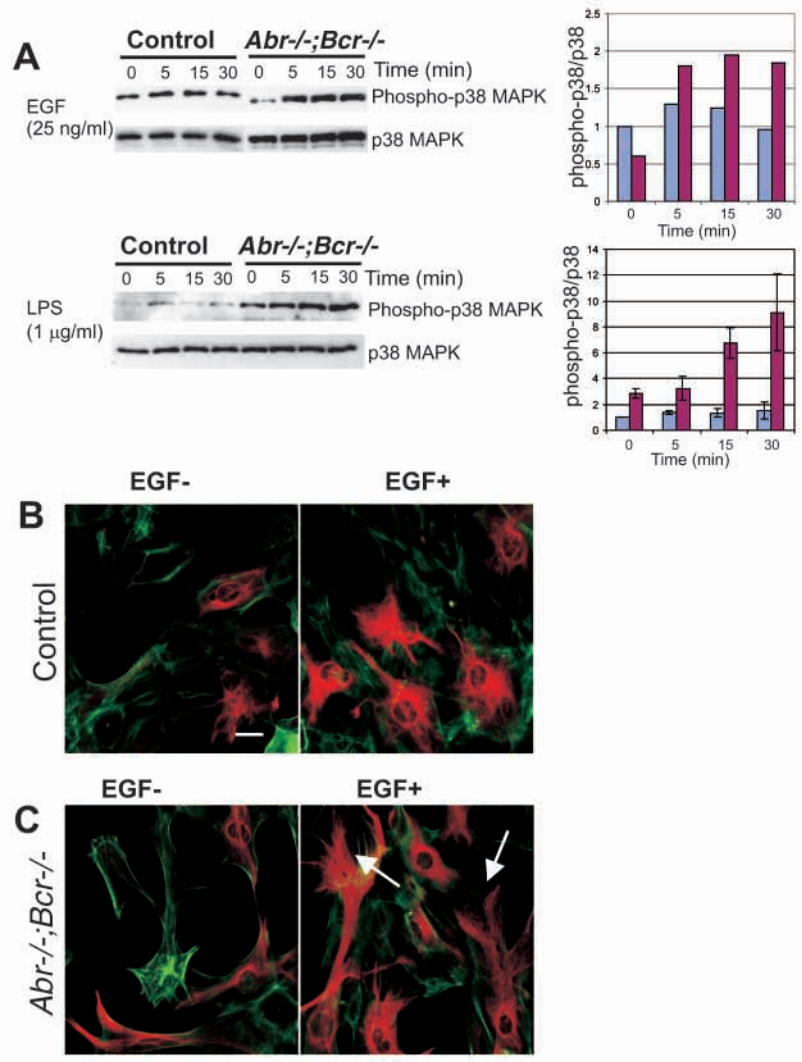

Fig. 8. Altered response to external stimuli in double null mutant cells. (A) Primary astrocytes were stimulated with EGF (25 ng/ml; upper panel) or LPS (1 μg/ml; lower panel) and analyzed for p38 MAPK phosphorylation using anti-phospho-p38 MAPK antibodies. The filters were subsequently stripped and probed with anti-p38 MAPK antibodies. The histograms to the right represent the relative quantitation of the scanned images. In the histograms, the wild-type (control) phospho-p38/p38 ratio without stimuli was arbitrarily set at 1 (upper histogram, average of two independent experiments; lower histogram, *n*=4, error bars indicate s.d.). Blue bars, wild-type samples; red bars, double null mutant samples. (B,C) Comparison of serum-starved and EGF-stimulated wild-type control and double null mutant primary astrocytes. Primary astrocytes from wild-type controls and double null mutants were serum-starved for 24 hours (left panels) or stimulated with EGF (25 ng/ml) for 24 hours (right panels). Astrocytes were identified by labeling for GFAP (red-Cy3), double stained for actin (green-FITC) and analyzed using confocal microscopy. Serum-starved null mutant astrocytes were more spread than controls. When stimulated with EGF, wild-type controls showed no morphological changes, whereas some $Abr^{-/-};Bcr^{-/-}$ astrocytes (arrows in C) responded with the projection of GFAP-positive protrusions. Scale bar: 20 μm.

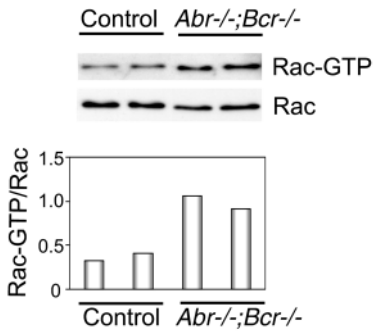

Fig. 9. Abrogation of Abr and Bcr causes increased levels of RacGTP. RacGTP was affinity-precipitated from lysates using GST-PAK (top panel). Levels of total Rac and RacGTP were evaluated using western blotting with anti-Rac antibodies. The lower panel represents the quantitation of scanned images. When compared with two wild-type controls, non-stimulated monocytes from two independent $Abr^{-/-};Bcr^{-/-}$ mutants showed approx. threefold higher levels of RacGTP.

mutant astrocytes responded to LPS stimulation with a very robust and progressively increasing phosphorylation of p38 MAPK, in comparison with controls, which showed a modest but detectable increase. Thus, these experiments demonstrate that Abr and Bcr together downregulate responses of astrocytes to extracellular stimuli, and that in the absence of these negative regulators of Rac in vivo, astrocytes react to stimuli by abnormal morphological responses and activation of the p38 MAPK pathway.

Loss of Abr and Bcr leads to Rac activation

As mentioned above, Bcr and Abr contain both a domain with demonstrated in vivo GAP activity against Rac and robust in vitro GAP activity against Rac and Cdc42, as well as a domain with very modest in vitro GEF activity. To examine whether the GEF domain has an in vivo function in cerebellar development, we generated transgenic mice that expressed a Bcr protein containing its entire N-terminal moiety, including the DH-PH (GEF) domain, but not the GAP domain, under the control of the BCR promoter. The expression level of the transgenic protein in the brain of these mice was comparable with that produced by a single endogenous *Bcr* allele. This transgenic strain was crossed with $Abr^{-/-};Bcr^{-/-}$ mice and breeding was continued until transgenic double knockout (Bcr-DH-PH; $Abr^{-/-};Bcr^{-/-}$) mice were obtained. A careful comparison between the double knockouts and transgenic double knockouts revealed that the expression of the Bcr-PH-DH protein was not able to rescue the cerebellar phenotype of double knockout mice (data not shown).

The GAP domains of Abr and Bcr act as negative regulators of RacGTP levels in vitro. Loss of such negative regulators in vivo would be predicted to result in increased levels of RacGTP. To investigate this, we examined the levels of RacGTP in monocytes, a cell type that is particularly suitable to address this question as it contains relatively high levels of Rac in comparison with other cells. As shown in Fig. 9, using a GST-Pak binding assay, we were able to show, for the first time in vivo, that ablation of *Bcr* and *Abr* affects endogenous levels of RacGTP. As compared with controls (wild-type and single null mutant mice), we detected approximately threefold higher levels of RacGTP in non-stimulated monocytes of double null mutants. By contrast, no changes in the levels of Cdc42 GTP were detected in the same samples (data not shown). Together, these results correlate the combined function of Abr and Bcr as RacGAPs to the regulation of Rac activity in vivo.

DISCUSSION

The current study demonstrates that the simultaneous disruption of two proteins that negatively regulate Rac in vivo leads to the appearance of ectopic granule cells and foliation defects in the postnatal murine cerebellum. This phenotype could be explained by defects in several guidance and support systems, which are in place for EGL cells, as well as in the EGL cells themselves. Despite extensive investigation, we were unable to find any supporting evidence for the possibility that the double null mutant granule cells would have intrinsic defects including altered migration. Nevertheless, we can not entirely rule out the possibility that a small abnormal subpopulation of granule cells exists, which would be partially responsible for the detected phenotype. Unfortunately, the isolation of this hypothetical population of granule cells from the pool of premigratory granule cells is not possible as we have no molecular markers for them. Although we failed to find any evidence either for defects in Purkinje cell structure and function, we could already detect disorganized radial glia and abnormal astroglia on the cerebellar cortex at P5, at locations where ectopic granule cells and foliation defects are subsequently found after completion of granule cell migration. The aberrant GFAP-positive astroglia on the pial surface possessed long Bergmann-like processes and they were in the right location to make contact with premigratory granule cells. These aberrant cells could affect adjacent premigratory granule cells either directly, by cell-cell contact, or indirectly, by secreting soluble factors. Either one or both of these effects would interfere with normal granule cell migration. This, in conjunction with the observed abnormal processes of a subset of the Bergmann glial cells themselves, is the most likely cause of the granule cell ectopia found in double null mutants.

The origin of Bergmann glia is still controversial. One possibility is, that they originate from either primordial radial glia or from non-radial glial cells, which migrate from the ventricular zone toward the cortex. Alternatively, they may derive from glial stem cells in the EGL, which migrate to the Purkinje cell plate, possibly guided by primordial radial glia that are already in place. We have detected aberrant GFAP and S100 positive cells in the EGL at p5. If these aberrant cells with long protrusions indeed represent abnormal Bergmann glial cells rather than other glial cells, this would favor the possibility that Bergmann cells originate in the EGL.

Experiments in which constitutively active Rac was overexpressed in cultured astrocytes have shown that astrocyte process formation and morphology is severely affected by the GTP-bound state of Rac (Kalman et al., 1999). Although the possible factors that trigger activation of Rac in vivo in astrocytes remain undetermined, there is evidence that at least under certain biological conditions, this signal is generated by neurons. For example, it has been shown that neurons stimulate

the growth of astrocyte processes in vitro (Gasser and Hatten, 1990). The finding that *Abr;Bcr* double null mutants show developmental defects in glial cell populations and respond to excitotoxic stimuli by developing severe gliosis, implies that in astrocytes *Abr* and *Bcr* together function as regulators of Rac-mediated pathways that sense external stimuli and induce morphological changes.

We further tested this possibility by analyzing both the baseline phosphorylation status of different members of the MAPK family, as well as their inducibility in *Abr;Bcr* double null mutant and control astrocytes. In the presence of serum, the *Abr;Bcr* double null mutant cells showed an approx. threefold higher baseline phosphorylation level of p38 MAPK, whereas ERK and JNK phosphorylation levels were similar to those of controls. Initially, the p38 MAPK was identified as participating in the transduction of signals involved in inflammation and was linked to transcriptional regulation. Subsequently, it became clear that this kinase mediates multiple different cellular responses, including those associated with migration and cytoskeletal reorganization, and that these responses were triggered by a wide variety of cytokines, growth factors and stress. As it has been demonstrated, that primary astrocytes respond to LPS by p38 MAPK phosphorylation (Schumann et al., 1998), we used LPS-mediated stimulation as a model to demonstrate a dramatic increase in the reactivity of the p38 MAPK pathway in *Abr;Bcr* mutants. Double mutant astrocytes were also more responsive to EGF stimulation, by displaying increased p38 phosphorylation. Our data are not fully in concordance with those published by Kalman and co-workers (Kalman et al., 1999). These authors showed that in hippocampal astrocytes, the effect of bFGF (and EGF) can be mimicked by dominant-negative Rac1 and RhoA, whereas activated mutants blocked and reversed growth factor effects. However, they also concluded that low levels of Rac1 and RhoA are required to initiate and maintain growth factor-induced processes. Thus, the more subtle changes in Rac activation in vivo are likely to be the explanation for discrepancies found between the studies using the dominant mutants and our null mutant studies, and provide novel insights into the role of these signaling molecules in astrocyte functions.

The pathways by which Rac is activated upon stimulation of receptor tyrosine kinases such as the EGF receptor have been studied extensively (Nimnual et al., 1998; Scita et al., 1999). By contrast, mechanisms by which Racs are downregulated are much less well defined. Our present results demonstrate that negative regulators of Rac have a crucial role in the regulation of proper development. Failure to downregulate activated Rac, caused by the ablation of essential GTPase activating proteins, can lead to abnormal responses of certain cells to extracellular stimuli in the context of the whole organism. In astrocytes, this leads to a hyper-reactivity in response to external stimuli and consequently to developmental defects. This has profound consequences for the development and function of the CNS.

We thank Hermien van Schaick for cloning of the murine *Abr* genomic DNA fragments, Karen Leung for assistance with genotyping, George McNamara (CHLARI Image Core) for assistance with confocal microscopy and Thomas Coates for helpful discussions. This work was supported by the T. J. Martell Foundation and PHS NIH grants HL60231 to J. G., CA50248 to N. H. and DE13085 to V. K.

REFERENCES

Allen, K. M., Gleeson, J. G., Bagrodi, S., Partington, M. W., MacMillan, J. C., Cerione, R. A., Mulley, J. C. and Walsh, C. A. (1998). PAK3 mutation in non-syndromic X-linked mental retardation. *Nat. Genet.* **20**, 25-30.

Angulo, A., Fernandez, E., Merchan, J. A. and Molina, M. (1996). A reliable method for Golgi staining for retina and brain slices. *J. Neurosci. Methods* **66**, 55-59.

Aderem, A. and Ulevitsh R. J. (2000). Toll-like receptors in the induction of the innate immune response. *Nature* **406**, 782-787.

Benard, V., Boh, B. P. and Bokoch, G. M. (1999). Characterization of rac and cdc42 activation in chemoattractant-stimulated human neutrophils using a novel assay for active GTPases. *J. Biol. Chem.* **274**, 13198-13204.

Billuart, P., Bienvenu, T., Ronce, N., des Portes, V., Vinet, M. C., Zemni, R., Crollius, H. R., Carrie, A., Fauchereau, F., Cherry, M. et al. (1998). Oligophrenin-1 encodes a rhoGAP protein involved in X-linked mental retardation. *Nature* **392**, 923-926.

Chuang, T-H., Xu, X., Kaartinen, V., Heisterkamp, N., Groffen, J. and Bokoch, G. M. (1995). Abr and Bcr are multifunctional regulators of the Rho GTP-binding protein family. *Proc. Natl. Acad. Sci. USA* **92**, 10282-10286.

Dahlstrand, J., Lardelli, M. and Lendahl, U. (1995). Nestin mRNA expression correlates with the central nervous system progenitor cell state in many, but not all, regions of developing central nervous system. *Dev. Brain Res.* **84**, 109-129.

Dahmane, N. and Ruiz-i-Altaba, A. (1999). Sonic hedgehog regulates the growth and patterning of the cerebellum. *Development* **126**, 3089-3100.

del Pozo, M. A., Price, L. S., Alderson, N. B., Ren, X. D. and Schwartz, M. A. (2000). Adhesion to the extracellular matrix regulates the coupling of the small GTPase Rac to its effector PAK. *EMBO J.* **19**, 2008-2014.

Fioretos, T., Voncken, J. W., Baram, T. Z., Kamme, F., Groffen, J. and Heisterkamp, N. (1995). Regional localization and developmental expression of the BCR gene in rodent brain. *Cell. Mol. Brain Res.* **41**, 97-102.

Galli, C., Meucci, O., Scorziello, A., Werge, T. M., Calissano, P. and Schettini, G. (1995). Apoptosis in cerebellar granule cells is blocked by high KCl, forskolin, and IGF-1 through distinct mechanisms of action: the involvement of intracellular calcium and RNA synthesis. *J. Neurosci.* **15**, 1172-1179.

Gasser, U. E. and Hatten, M. E. (1990). Neuron-glia interactions of rat hippocampal cells in vitro: glial-guided neuronal migration and neuronal regulation of glial differentiation. *J. Neurosci.* **10**, 1276-1285.

Goldowitz, D. and Hamre, K. (1998). The cells and molecules that make a cerebellum. *Trends Neurosci.* **21**, 375-382.

Groffen, J. and Heisterkamp, N. (1997). The chimeric BCR-ABL gene. *Baillieres Clin. Haematol.* **10**, 187-201.

Hall, A. (1998). Rho GTPases and the actin cytoskeleton. *Science* **279**, 509-512.

Hatten, M. E. (1985). Neuronal regulation of astroglial morphology and proliferation in vitro. *J. Cell Biol.* **100**, 384-396.

Hatten, M. E. (1990). Riding the glial monorail: a common mechanism for glial-guided neuronal migration in different regions of the developing mammalian brain. *Trends Neurosci.* **13**, 179-184.

Heisterkamp, N., Kaartinen, V., van Soest, S., Bokoch, G. M. and Groffen, J. (1993). Human ABR encodes a protein with GAPrac activity and homology to the dbl nucleotide exchange factor domain. *J. Biol. Chem.* **268**, 16903-16906.

Kaartinen, V., Voncken, J. W., Shuler, C., Warburton, D., Bu, D., Heisterkamp, N. and Groffen, J. (1995). Abnormal lung development and cleft palate in mice lacking TGF-β3 indicates defects of epithelial-mesenchymal interaction. *Nat. Genet.* **11**, 415-420.

Kalman, D., Gomperts, S. N., Hardy, S., Kitamura, M. and Bishop, J. M. (1999). Ras family GTPases control growth of astrocyte processes. *Mol. Biol. Cell* **10**, 1665-1683.

Kornblum, H. I., Hussain, R., Wiesen, J., Miettinen, P., Zurcher, S. D., Chow, K., Derynck, R. and Werb, Z. (1998). Abnormal astrocyte development and neuronal death in mice lacking the epidermal growth factor receptor. *J. Neurosci. Res.* **53**, 697-717.

Kraynov, V. S., Chamberlain, C., Bokoch, G. M., Schwartz, M. A.,

Slabaugh, S. and Hahn, K. M. (2000). Localized rac activation dynamics visualized in living cells. Science **290**, 333-337.

Kutsche, K., Yntema, H., Brandt, A., Jantke, I., Gerd Nothwang, H., Orth, U., Boavida, M. G., David, D., Chelly, J., Fryns, J. P. et al. (2000). Mutations in ARHGEF6, encoding a guanine nucleotide exchange factor for rho GTPases, in patients with X-linked mental retardation. *Nat. Genet.* **2**, 247-250.

Luo, L., Hensch, T. K., Ackerman, L., Barbel, S., Jan, L. Y. and Jan, Y. N. (1996). Differential effects of the Rac GTPase on Purkinje cell axons and dendritic trunks and spines. *Nature* **379**, 837-840.

Mission, J. P., Edwards, M. A., Yamamoto, M. and Caviness, V. S., Jr (1988). Identification of radial glial cells within the developing murine central nervous system: studies based upon a new immunohistochemical marker. *Dev. Brain Res.* **44**, 95-108.

Mueller, B. K. (1999). Growth cone guidance: First steps towards a deeper understanding. *Annu. Rev. Neurosci.* **22**, 351-388.

Nimnual, A. S., Yatsula, B. A. and Bar-Sagi, D. (1998). Coupling of Ras and Rac guanosine triphosphatases through the Ras exchanger Sos. *Science* **279**, 560-563.

O'Neill, L. (2000) The Toll/interleukin-1 receptor domain: a molecular switch for inflammation and host defense. *Biochem. Soc. Trans.* **28**, 557-563.

Robinson, K. A., Stewart, C. A., Pye, Q. N., Nguyen, X., Kenney, L., Salzman, S., Floyd, R. A. and Hensley, K. (1999). Redox-sensitive protein phosphatase activity regulates the phosphorylation state of p38 protein kinase in primary astrocyte culture. *J. Neurosci. Res.* **55**, 724-732.

Scita, G., Nordstrom, J., Carbone, R., Tenca, P., Giardina, G., Gutkind, S., Bjarnegard, M., Betsholtz, C. and Di Fiore, P. P. (1999). EPS8 and E3B1 transduce signals from Ras to Rac. *Nature* **401**, 290-293.

Schumann, R., Pfeil, D., Freyer, D., Buerger, W., Lamping, N., Kirschning, C. J., Goebel, U. B. and Weber, J. R. (1998). Lipopolysaccharide and pneumococcal cell wall components activate the mitogen activated protein kinases (MAPK) erk1, erk2 and p38 in astrocytes. *Glia* **22**, 295-305.

Spector, D. L., Goldman, R. D. and Leinwand, L. A. (1997). Plasmamembrane changes during cell death. In *Cells. A Laboratory Manual* (ed. D. L. Spector, R. D. Goldman and L. A. Leinwand), pp 15.8-15.10. Cold Spring Harbor: Cold Spring Harbor Laboratory Press.

Tan, E. C., Leung, T., Manser, E. and Lim, L. (1993). The human active breakpoint cluster region-related gene encodes a brain protein with homology to guanine nucleotide exchange proteins and GTPase-activating proteins. *J. Biol. Chem.* **268**, 27291-27298.

van Aelst, L. and D'Souza-Schorey, C. (1997). Rho GTPases and signaling networks. *Genes Dev.* **11**, 2295-2322.

van Essen, D. C. (1997). A tension-based theory of morphogenesis and compact wiring in the central nervous system. *Nature* **385**, 313-318.

von Knebel Doeberitz, C., Sievers, J., Sadler, M., Pehlmann, F.-W., Berry, M. and Halliwell, P. (1986). Destruction of meningeal cells over the newborn hamster cerebellum with 6-hydroxydopamine prevents foliation and lamination in the rostral cerebellum. *Neuroscience* **17**, 409-426.

Voncken, J.-W., van Schaick, H., Kaartinen, V., Deemer, K., Coates, T., Landing, B., Pattengale, P., Dorseuil, O., Bokoch, G. M., Groffen, J. and Heisterkamp, N. (1995). Increased neutrophil respiratory burst in bcr-null mutants. *Cell* **80**, 719-728.

Wechsler-Reya, R. J. and Scott, M. P. (1999). Control of neuronal precursor proliferation in the cerebellum by Sonic Hedgehog. *Neuron* **1**, 103-114.

Wurst, W. and Joyner, A. (1993). Production of targeted embryonic stem cell clones. In *Gene Targeting: A Practical Aproach* (ed. A. L. Joyner), pp. 31-62. Oxford: Oxford University Press.

Yuasa, S. (1996). Bergmann glial development in the mouse cerebellum as revealed by tenascin expression. *Anat. Embryol.* **194**, 223-234.